Osteoclast precursors in murine bone marrow express CD27 and are impeded in osteoclast development by CD70 on activated immune cells

Yanling Xiao[a,1], Ji-Ying Song[b], Teun J. de Vries[c,d], Christien Fatmawati[a], Diana B. Parreira[a], Geerling E. J. Langenbach[c,d], Nikolina Bąbała[a], Martijn A. Nolte[e], Vincent Everts[c,d], and Jannie Borst[a,1]

[a]Division of Immunology and [b]Department of Animal Pathology, The Netherlands Cancer Institute, 1066 CX, Amsterdam, The Netherlands; Departments of [c]Periodontology and [d]Oral Cell Biology and Functional Anatomy, Academic Centre for Dentistry Amsterdam, 1081 LA, Amsterdam, The Netherlands; and [e]Department of Hematopoiesis, Sanquin Research, 1066 CX, Amsterdam, The Netherlands

Edited by Joseph Lorenzo, University of Connecticut Health Center, Farmington, CT, and accepted by the Editorial Board June 6, 2013 (received for review September 29, 2012)

Osteoclasts (OCs) are bone-resorbing cells that are formed from hematopoietic precursors. OCs ordinarily maintain bone homeostasis, but they can also cause major pathology in autoimmune and inflammatory diseases. Under homeostatic conditions, receptor activator of nuclear factor kappa-B (RANK) ligand on osteoblasts drives OC differentiation by interaction with its receptor RANK on OC precursors. During chronic immune activation, RANK ligand on activated immune cells likewise drives pathogenic OC differentiation. We here report that the related TNF family member CD70 and its receptor CD27 can also mediate cross-talk between immune cells and OC precursors. We identified CD27 on a rare population (0.3%) of B220$^-$c-Kit$^+$CD115$^+$CD11b^{low} cells in the mouse bone marrow (BM) that are highly enriched for osteoclastogenic potential. We dissected this population into CD27^{high} common precursors of OC, dendritic cells (DCs) and macrophages and CD27$^{low/neg}$ downstream precursors that could differentiate into OC and macrophages, but not DC. In a recombinant mouse model of chronic immune activation, sustained CD27/CD70 interactions caused an accumulation of OC precursors and a reduction in OC activity. These events were due to a CD27/CD70-dependent inhibition of OC differentiation from the OC precursors by BM-infiltrating, CD70$^+$-activated immune cells. DC numbers in BM and spleen were increased, suggesting a skewing of the OC precursors toward DC differentiation. The impediment in OC differentiation culminated in a high trabecular bone mass pathology. Mice additionally presented anemia, leukopenia, and splenomegaly. Thus, under conditions of constitutive CD70 expression reflecting chronic immune activation, the CD27/CD70 system inhibits OC differentiation and favors DC differentiation.

hematopoiesis | osteoimmunology | costimulation | TNF receptor family

Bone homeostasis relies on the balance between bone-forming osteoblasts (OBs) and bone-degrading osteoclasts (OCs). Whereas OBs are derived from mesenchymal stem cells (1), OCs are hematopoietic cells of the myeloid lineage (2). The cytokines macrophage-colony stimulating factor (M-CSF) and receptor activator of nuclear factor kappa-B (RANK) ligand (L) drive OC development from their bone marrow (BM) precursors. M-CSF mediates proliferation and survival of OC precursors (P) (3) and stimulates OCPs to express the receptor for RANKL (2). RANKL promotes the differentiation of OCPs into mature OCs (4–6) and activates mature OCs to resorb bone (7). Under homeostatic conditions, RANKL is produced by OBs (4, 8) and osteocytes (9), but, in chronic immune activation or autoimmunity, RANKL can also be produced by immune cells that thereby cause pathological bone loss and remodeling (10–12).

OCs are derived from myeloid progenitors that also give rise to monocytes, macrophages, and dendritic cells (DCs). However, the phenotypic definitions of OCP are remarkably varied. OCs are derived experimentally from total BM or subpopulations thereof, but also from committed immature DCs, monocytes, or macrophages. In the mouse, a common precursor of OCs and DCs has been identified in the BM (2, 13), in a cell population that expresses the Stem-Cell Factor receptor c-Kit, the M-CSF receptor CD115, and the myeloid lineage marker CD11b (at low level). In this study, we identify CD27 as a marker that discriminates these c-Kit$^+$CD115$^+$CD11b^{low} common OC/DC precursors from their still RANK-negative, but more OC-committed, offspring. In the mouse, CD27 is expressed on hematopoietic stem cells (14), common lymphoid (15, 16), myeloid, and granulocyte/macrophage progenitors (17). CD27 is not required for hematopoiesis under homeostatic conditions but regulates responses of mature T and B lymphocytes upon infection or immunization (18, 19).

CD27 provides costimulatory signals for survival of activated lymphocytes (18, 19). CD27 costimulation is critical for virus control in human, as testified by the lethal EBV viremia in human genetic CD27 deficiency (20). CD27 function is controlled by the tightly regulated expression of its ligand CD70. CD70 is an exquisite hallmark of an activated immune system. It is induced on DCs and B and T cells upon their activation (18, 19). In rheumatoid arthritis patients, CD70 is the most important differentially expressed gene in CD4$^+$ T cells (21). CD70 expression on CD4$^+$ T cells is diagnostics in systemic lupus erythematosus (22). CD70 expression not only hallmarks chronic immune activation, but it also drives this process. In mice with constitutive, transgenic CD70 expression on B cells or DC, the threshold for T-cell activation is lowered. As a result, effector CD4$^+$ and CD8$^+$ T cells are generated in the absence of deliberate immunization. Also, endogenous CD70 expression is induced on a variety of activated immune cells (19, 23, 24).

We report here that mice suffering from chronic immune activation due to constitutive expression of CD70 on DCs develop a CD27-dependent high trabecular bone mass pathology. These mice have reduced OC activity whereas bone-forming activity appeared normal. We found that CD27 is expressed on B220$^-$c-Kit$^+$CD115$^+$CD11b^{low} OCPs in the BM of healthy mice and diagnoses two successive stages of OC commitment. In the affected mice, endogenous CD70 on BM-infiltrating activated immune cells inhibited OC differentiation from these OCPs, in

Author contributions: Y.X. and J.B. designed research; Y.X., J.-Y.S., C.F., D.B.P., and N.B. performed research; T.J.d.V., G.E.J.L., M.A.N., and V.E. contributed new reagents/analytic tools; Y.X., G.E.J.L., T.J.d.V., and J.B. analyzed data; and Y.X. and J.B. wrote the paper.

The authors declare no conflict of interest.

Freely available online through the PNAS open access option.

This article is a PNAS Direct Submission. J.L. is a guest editor invited by the Editorial Board.

[1]To whom correspondence may be addressed. E-mail: j.borst@nki.nl or y.xiao@nki.nl.

This article contains supporting information online at www.pnas.org/lookup/suppl/doi:10.1073/pnas.1216082110/-/DCSupplemental.

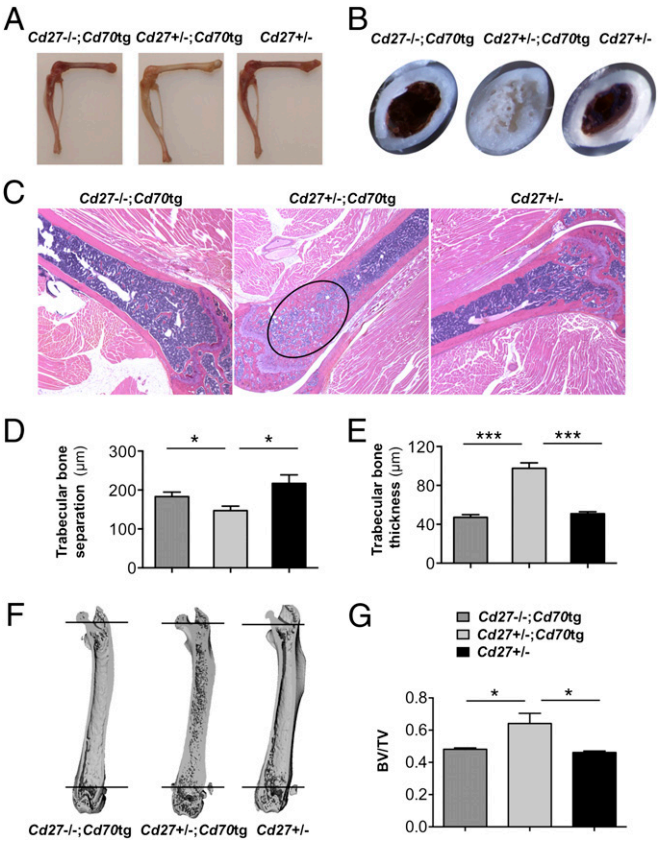

Fig. 1. *Cd27*$^{+/-}$;*Cd70*tg mice have a high trabecular bone mass phenotype. (*A*) Macroscopic view of pale bone in *Cd27*$^{+/-}$;*Cd70*tg mice, compared with *Cd27*$^{-/-}$;*Cd70*tg and *Cd27*$^{+/-}$ control mice. (*B*) Stereomicroscopy of long bones from mice of the indicated genotypes. (*C*) Examples of histological analyses of long bones from mice of the indicated genotypes (age 10–12 wk). Oval denotes the affected area in *Cd27*$^{+/-}$;*Cd70*tg mice. (Original magnification: 2.5×.) High magnifications of deeper sections of the same bones (10×) are shown in Fig. S1*A*. (*D* and *E*) Quantification of trabecular bone separation and thickness from histological data of male mice (age 8–10 wk; *Cd27*$^{-/-}$;*Cd70*tg: $n = 3$; *Cd27*$^{+/-}$;*Cd70*tg: $n = 5$; *Cd27*$^{+/-}$ $n = 4$; $*P < 0.05$; $**P < 0.01$; $***P < 0.001$). See Fig. S1 *B* and *C* for data on female mice and Fig. S1*D* for BV/TV. (*F*) Illustration of the high trabecular bone mass phenotype by μCT. Region between the two lines was used for BV/TV determination on total tibia, including trabecular and cortical bone. (*G*) Quantification of BV/TV (ratio) from μCT data in age-matched mice of the indicated genotypes ($n = 3$–4, $*P < 0.05$).

a CD27-dependent manner. This inhibition explained the high bone mass phenotype and revealed a pathway of CD27/CD70-mediated control on osteoclastogenesis.

Results

High Trabecular Bone Mass and Repressed Hematopoiesis in CD11c-*Cd70*tg Mice. To create a model of chronic immune activation, CD70 was constitutively expressed on conventional DCs under control of the CD11c promoter (24). The resulting CD11c-*Cd70* transgenic (tg) line was maintained on a CD27-deficient background by interbreeding of *Cd27*$^{-/-}$;*Cd70*tg mice. This breeding was done to avoid immune activation due to constitutive CD27–CD70 interactions. To generate CD27-proficient *Cd70*tg mice, the *Cd27*$^{-/-}$;*Cd70*tg mice were bred with WT mice, resulting in *Cd27*$^{+/-}$;*Cd70*tg and *Cd27*$^{+/-}$ littermates. We consistently observed that the *Cd27*$^{+/-}$;*Cd70*tg mice had abnormally pale bones, compared with *Cd27*$^{-/-}$;*Cd70*tg and *Cd27*$^{+/-}$ control mice (Fig. 1*A*). Stereomicroscopy revealed that the bone cavity of these mice was aberrantly filled with trabecular bone (Fig. 1*B*). Histological examination of 8- to 21-wk-old mice confirmed that the bone cavity of *Cd27*$^{+/-}$;*Cd70*tg mice was aberrantly filled with trabecular bone, particularly in the metaphysis near the growth plate (Fig. 1*C*, Fig. S1*A*). This pathology was apparent in long bones and sternum of *Cd27*$^{+/-}$;*Cd70*tg mice, regardless of sex. Quantitative analysis of histological images pointed out that, in both males and females, trabecular bone separation was significantly reduced (Fig. 1*D*, Fig. S1*B*) and trabecular bone thickness (Fig. 1*E*, Fig. S1*C*) was significantly increased in *Cd27*$^{+/-}$;*Cd70*tg mice, compared with control mice. The bone area per tissue area (BV/TV) as deduced from histology was significantly higher (Fig. S1*D*). Femurs were also examined by high-resolution microcomputed tomography (μCT), as illustrated in Fig. 1*F*. The μCT analysis confirmed the histological findings. In *Cd27*$^{+/-}$;*Cd70*tg mice, the trabecular bone was increased in volume and in places fused with the cortical bone. Quantitative analysis of the μCT data indicated that the BV/TV for total tibia, including both trabecular and cortical bone, was significantly higher in *Cd27*$^{+/-}$;*Cd70*tg mice than in control mice (Fig. 1*G*).

In the time frame of 4–11 wk after birth, *Cd27*$^{+/-}$;*Cd70*tg mice, but not control mice, developed additional pathology in the form of leukopenia, anemia (Fig. S2*A*), and enlarged spleens (Fig. S2*B*) with increased hematopoietic activity (Fig. S2*C*). We conclude that *Cd27*$^{+/-}$;*Cd70*tg mice develop a high trabecular bone mass pathology and repressed hematopoiesis. The disease phenotype in CD11c-*Cd70*tg mice is driven by constitutive CD27–CD70 interactions because it does not appear when CD70 is constitutively expressed on a CD27-deficient background.

Bone Formation Appears Normal in CD11c-*Cd70*tg Mice. The increased trabecular bone mass in *Cd27*$^{+/-}$;*Cd70*tg mice could be due to

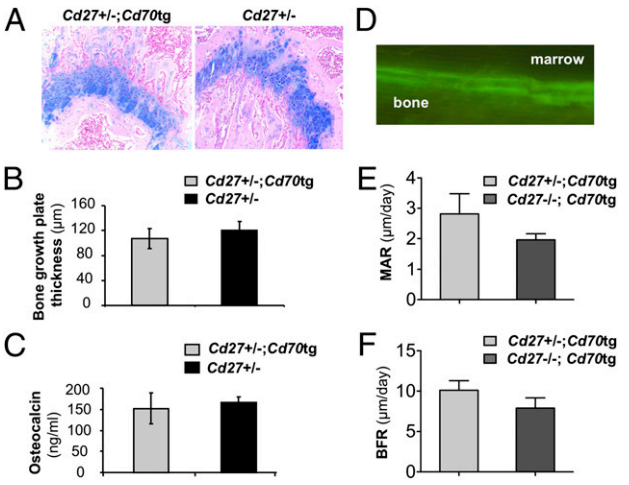

Fig. 2. Bone forming activity appears normal in *Cd27*$^{+/-}$;*Cd70*tg mice. (*A*) Alcian blue-periodic acid Schiff histochemistry, identifying cartilage extracellular matrix within the growth plate of the femur. (Original magnification: 20×.) (*B*) Using ImageJ software, histochemistry data were quantified in *Cd27*$^{+/-}$;*Cd70*tg and *Cd27*$^{+/-}$ control mice ($n = 5$; age 10–12 wk). (*C*) Serum level of the bone formation marker osteocalcin, determined by ELISA in *Cd27*$^{+/-}$;*Cd70*tg mice and *Cd27*$^{+/-}$ control mice ($n = 8$; age 8–10 wk). (*D*–*F*) Dynamic bone labeling with calcein of female *Cd27*$^{+/-}$;*Cd70*tg mice and control *Cd27*$^{-/-}$;*Cd70*tg mice ($n = 3$–4; age 8 wk). Mice were injected at days 0 and 7 with 10 mg/kg calcein (Sigma) in PBS and killed at day 10. Longitudinal midfemur cryostat sections from snap frozen, gelatin-embedded bones were analyzed by microscopy. (*D*) Illustration of calcein incorporation into the femur shaft bone as detected by fluorescence microscopy. Dynamic bone parameters were assessed for half of the shaft. (*E*) Mineral apposition rate (MAR), determined by measuring the distance between the two fluorescent lines depicted in *D* at multiple sites in the shaft and calculating the mean. (*F*) Bone formation rate (BFR), i.e., MAR multiplied by the shaft fraction that was double labeled with calcein, based on half of the shaft length, measured from the epiphysis.

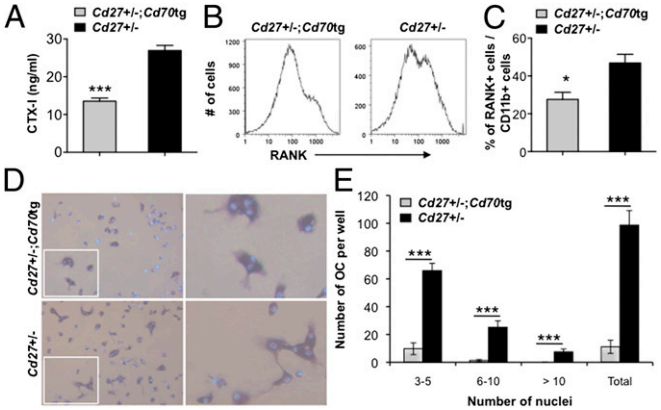

Fig. 3. OC differentiation is reduced in *Cd27*$^{+/-}$*;Cd70*tg mice. (*A*) CTX-I levels, read out by ELISA in serum of *Cd27*$^{+/-}$*;Cd70*tg mice and *Cd27*$^{+/-}$ control mice ($n = 5$; age 12 wk). The experiment is representative of two. (*B* and *C*) RANK induction. Total BM of *Cd27*$^{+/-}$*;Cd70*tg mice and *Cd27*$^{+/-}$ control mice ($n = 4$) was cultured for 3 d with M-CSF and analyzed for presence of RANK$^+$, CD11b$^+$ cells. (*B*) Representative flow cytometric analysis. (*C*) Quantification of RANK$^+$ cells within CD11b$^+$ BM cells. (*D* and *E*) Total BM cells of 7- to 8-wk-old mice ($n = 4$) were cultured at 100,000 cells per well in duplicate with M-CSF and RANKL. At day 6, mature OCs were identified as tartrate-resistant acid phosphatase (TRAP)$^+$ cells containing more than three nuclei. (*D*) Microscopic image of in vitro OC differentiation cultures showing TRAP and DAPI staining. *Insets* in *Left* indicate areas selected for digital zoom-ins presented in *Right*. (*E*) Quantitative analysis of OC differentiation. OCs are categorized in classes with 3–5, 6–10, and more than 10 nuclei (***$P < 0.001$). Data are representative of multiple independent experiments.

increased bone formation and/or to decreased bone degradation. We assessed thickness of the bone growth plate by alcian blue histochemistry (Fig. 2*A*). The growth plate consists of cartilage that is partly mineralized by newly deposited bone. The thickness of the growth plate was similar in *Cd27*$^{+/-}$*;Cd70*tg mice and *Cd27*$^{+/-}$ controls (Fig. 2*B*), giving no indication for altered bone formation. Furthermore, levels of osteocalcin, a serum marker of bone formation, were comparable in *Cd27*$^{+/-}$*;Cd70*tg mice and in controls (Fig. 2*C*). Dynamic bone formation was assessed by in vivo labeling with calcein (Fig. 2*D*). No statistically significant differences were detected between *Cd27*$^{+/-}$*;Cd70*tg mice and *Cd27*$^{-/-}$*;Cd70*tg controls in mineral apposition rate (MAR) (Fig. 2*E*) and bone formation rate (BFR) (Fig. 2*F*). Therefore, the bone phenotype in *Cd27*$^{+/-}$*;Cd70*tg mice was most likely not due to increased OB number and/or activity.

OC Function Is Diminished in CD11c-*Cd70*tg Mice. Serum levels of collagen type I telopeptides (CTX-I) were significantly lower in *Cd27*$^{+/-}$*;Cd70tg* mice than in *Cd27*$^{+/-}$ controls (Fig. 3*A*), suggesting a deficit in OC activity and/or formation. Upon in vitro culture with M-CSF, BM cells of *Cd27*$^{+/-}$*;Cd70*tg mice were slower or less effective to generate CD11b$^+$RANK$^+$ cells than BM cells of *Cd27*$^{+/-}$ control mice (Fig. 3 *B* and *C*). BM cells were next cultured with M-CSF and RANKL, and generation of multinuclear OC was determined as described (25) (Fig. 3*D*). In *Cd27*$^{+/-}$*;Cd70*tg BM cultures, the yield of OC was significantly lower than in control *Cd27*$^{+/-}$ cultures, in all categories of multinucleated cells (Fig. 3*E*). We conclude that BM precursors in *Cd27*$^{+/-}$*;Cd70*tg mice have a diminished capacity to differentiate into OC, which is linked with reduced overall OC activity. Impaired OC differentiation is the probable cause of the high trabecular bone mass phenotype in these mice because OB function appeared normal.

CD27 Hallmarks OCPs and Separates Them into Common OC/DC Precursors and More Committed OCPs. To examine how OC differentiation was affected, it was important to assess the frequency and differentiation potential of OCPs. Reportedly, OCPs reside in the B220$^-$CD11b^{low} subset of c-Kit$^+$CD115$^+$ hematopoietic precursor cells (2, 13, 26). To verify this concept, we sorted c-Kit$^+$CD115$^+$ BM cells into B220$^+$ or B220$^-$ cells that were either CD11b^{high} or CD11b^{low} (Fig. S3*A*). The B220$^+$ populations failed to give rise to OCs upon in vitro culture, but both B220$^-$ populations yielded OCs, with the CD11b^{low} population being the most effective (Fig. S3 *B* and *C*). This observation confirmed that a B220$^-$c-Kit$^+$CD115$^+$CD11b^{low} phenotype specifies OCPs in the mouse BM. Strikingly, CD27 was expressed on these OCPs (Fig. 4*A*, *Left*), and the CD27 expression level discerned CD27^{high} (G2) and CD27^{low} (G1) subsets within the OCP population. The combined subsets comprised less than 0.4% of total BM cells (Fig. 4*A*, *Right*). Recently, a CD115$^+$RANK$^+$ OCP has been described (27). Flow cytometry indicated that this population is most likely a subset of the CD27^{low} OCPs that are partly RANK$^+$ (Fig. S4*A*). CD27^{high} OCPs did not have RANK expression (Fig. S4*A*), suggesting that these are precursors

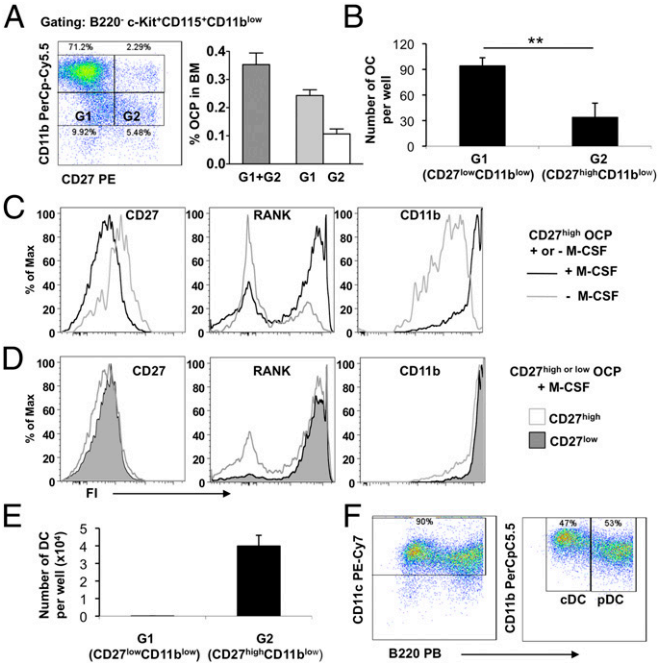

Fig. 4. CD27 is expressed on B220$^-$c-Kit$^+$CD115$^+$CD11b^{low} OCPs and separates them into common OC/DC precursors and more committed OCPs. (*A*, *Left*) Staining and gating strategy for flow cytometric identification of CD27 on B220$^-$c-Kit$^+$CD115$^+$CD11b^{low} OCPs in the murine BM, and subdivision of this population into CD27^{high} (G2) and CD27^{low} (G1) subsets. Numbers indicate the percentage of cells within the gate. Fluorochromes used were CD27 PE, B220 PB, c-Kit PE-Cy7, CD115 APC, and CD11b PerCP-Cy5.5. (*Right*) Frequency of indicated OCPs in total BM. (*B*) OCPs (B220$^-$c-Kit$^+$CD115$^+$CD11b^{low}) with a CD27^{high} (G2) or CD27^{low} (G1) phenotype were sorted from pooled BM cells of WT mice ($n = 4$), and 3,000 cells of each population were cultured under OC differentiation conditions. Triplicate cultures were quantified on day 5, (**$P < 0.01$). (*C* and *D*) Sorted CD27^{high} and CD27^{low} OCP subsets were cultured with (+) or without (–) M-CSF. After 36 h, CD27, RANK, and CD11b expression was determined by flow cytometry. (*E* and *F*) Sorted CD27^{high} and CD27^{low} OCP subsets were cultured with Flt3 ligand. At day 8, cells were stained for CD11c and B220 to identify conventional (c) DC and plasmacytoid (p) DC and analyzed by flow cytometry. (*E*) Quantification of total CD11c$^+$ DCs generated from CD27^{high} (G2) and CD27^{low} (G1) OCP subsets. (*F*) Representative flow cytometric analysis of cells derived from the CD27^{high} (G2) OCP subset, diagnosing cDCs, and pDCs. Data are representative of three independent experiments.

IMMUNOLOGY

of the CD27^{low} OCP. The CD27^{high} and CD27^{low} OCP subsets were purified by flow cytometric sorting (Fig. S4 *B* and *C*) and cultured under OC differentiation conditions. In the CD27^{low} OCP cultures (G1), mature OCs had developed at day 5 whereas significantly fewer OCs were seen in the CD27^{high} OCP cultures (G2) (Fig. 4*B*). To test the relationship between the CD27^{high} and CD27^{low} OCPs, we stimulated them with M-CSF that is known to up-regulate RANK on c-Kit^{+}CD115^{+}CD11b^{low} OCPs (2). M-CSF up-regulated RANK and CD11b expression on CD27^{high} OCPs and down-regulated CD27 expression (Fig. 4*C*, Fig. S4*D*). M-CSF did not alter CD27 expression on CD27^{low} OCPs. In the time frame of the assay, M-CSF more pronouncedly up-regulated RANK and CD11b on CD27^{low} OCPs than on CD27^{high} OCPs (Fig. 4*D*). These data suggest that the CD27^{high} OCP is the precursor of the CD27^{low} OCP.

OCs and DCs are closely related and can be derived from Fms-like tyrosine kinase 3 (Flt3)$^{+}$ common precursors (13). To test the potency of CD27^{high} and CD27^{low} OCPs to form DCs, they were cultured with Flt3 ligand. Only CD27^{high} OCPs, but not CD27^{low} OCPs could give rise to conventional and plasmacytoid DCs (Fig. 4 *E* and *F*). These data identify CD27 as a unique marker to discern successive stages of OC commitment in OCPs. The CD27^{high} B220^{-}c-Kit^{+}CD115^{+}CD11b^{low} BM cells are common precursors of OCs and DCs whereas their CD27^{low} offspring constitutes a population that can differentiate into OCs, but not DCs. It is known that c-Kit^{+}CD115^{+}CD11b^{low} OCPs can differentiate into OCs, DCs, and macrophages (2, 13). Both CD27^{high} and CD27^{low} OCPs could give rise to macrophages upon culture with M-CSF only (Fig. S4 *E* and *F*), so the CD27^{low} OCP is not fully committed to OC differentiation.

Sustained CD27–CD70 Interactions Prevent OCPs to Differentiate into OCs. We next examined the fate of the defined OCPs in *Cd27*$^{+/-}$;*Cd70*tg mice. In control *Cd27*$^{+/-}$ mice, the CD27^{high} and CD27^{low} OCPs were readily identified among B220^{-}c-Kit^{+}CD115^{+}CD11b^{low} BM cells (Fig. 5*A*). However, in *Cd27*$^{+/-}$;*Cd70*tg mice, the level of CD27 expression on these OCP was greatly reduced, approximating the background on *Cd27*$^{-/-}$;*Cd70*tg OCP (Fig. 5*A*). This expression level suggested that CD27 was down-regulated from the cell surface due to contact with CD70-bearing cells. The frequency (Fig. 5*B*) and absolute number (Fig. 5*C*) of total B220^{-}c-Kit^{+}CD115^{+}CD11b^{low} OCPs in the BM was significantly increased in *Cd27*$^{+/-}$;*Cd70*tg mice compared with *Cd27*$^{+/-}$ mice (Fig. 5*C*), indicating that constitutive CD27–CD70 interactions led to an OCP accumulation. In *Cd27*$^{-/-}$;*Cd70*tg mice, the frequency and absolute number of OCPs were comparable with those in *Cd27*$^{+/-}$ mice, indicating that CD27–CD70 interactions are not required for homeostatic OCP development or maintenance (Fig. 5 *B* and *C*). For comparison of their developmental potential, we cultured side-by-side total BM cells (at 100,000 cells per well) and sorted B220^{-}c-Kit^{+}CD115^{+}CD11b^{low} OCP (at 3,000 cells per well). The results at day 6 highlight the efficiency of OC formation from the sorted OCP that yielded more and larger multinucleated mature OCs in this time frame than the precursors in total BM (Fig. 5*D*, Fig. S5). OC formation from total BM cells of *Cd27*$^{+/-}$;*Cd70*tg mice was significantly impeded compared with the controls (Fig. 5*E*). Importantly, however, OC formation from purified OCPs was comparable between all three genotypes (Fig. 5*F*). This result indicated that, in *Cd27*$^{+/-}$;*Cd70*tg mice, OCPs cannot effectively differentiate into OCs due to contact with other cells in their BM environment. Apparently, sustained CD27–CD70 interactions between CD27-bearing OCPs and surrounding CD70-expressing cells inhibit the OCPs to differentiate into mature OCs.

Constitutive CD27 Engagement by CD70-Bearing Cells in the BM Limits OC Formation, But Allows DC Formation. We next set out to identify CD70-bearing cells in the BM that might be involved in interaction with CD27 on OCPs and inhibition of OC differentiation.

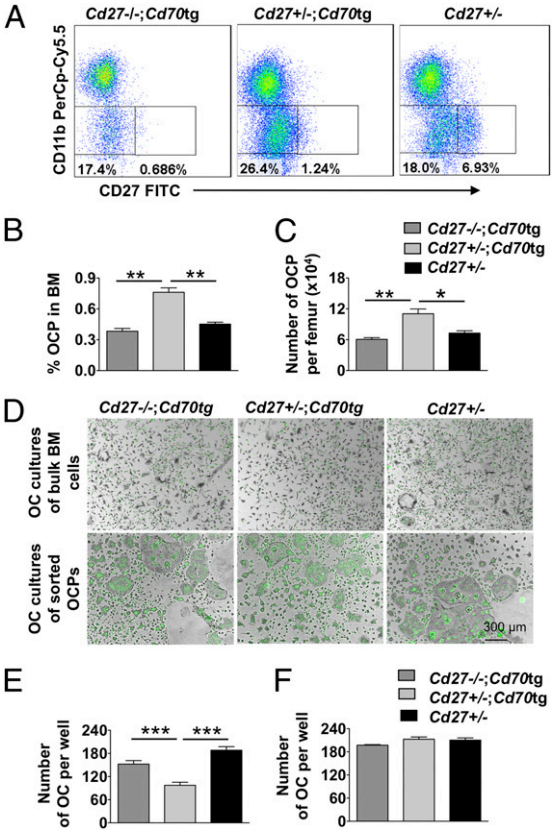

Fig. 5. Sustained CD27–CD70 interactions result in accumulation of CD27^{low} OCP in the BM that are arrested in their further development. (*A*) Flow cytometric analysis of CD27 expression levels on gated B220^{-}c-Kit^{+}CD115^{+} CD11b^{low} OCPs as identified in BM of mice of the indicated genotypes. Fluorochromes used were CD27 FITC, B220 PB, c-Kit PE-Cy7, CD115 APC, and CD11b PerCP-Cy5.5. (*B* and *C*) Frequency (*B*) and absolute number (*C*) of total B220^{-}c-Kit^{+}CD115^{+}CD11b^{low} OCPs in BM of mice of the indicated genotypes (n = 3–4; $^{*}P < 0.05$; $^{**}P < 0.01$). Data are representative of three independent experiments. (*D–F*) Side-by-side OC differentiation cultures of bulk BM cells and sorted OCPs. Bulk BM cells from mice of the indicated genotypes (n = 4, age 5 wk) were seeded at 100,000 cells per well. The same batches of BM cells were pooled (n = 4) per genotype for OCP sorting, and purified OCPs were seeded at 3,000 cells per well. Cultures were performed in quadruplicate and read out at day 6. (*D*) Representative images obtained by combined light and fluorescence microscopic examination of OC culture results at day 6. Green color represents DAPI staining of nuclei. (Original magnification: 5×.) (*E* and *F*) Quantification of OC numbers at day 6 after plating under OC culture conditions of bulk BM cells (*E*) or purified OCPs (*F*) ($^{***}P < 0.001$). Data are representative of two independent experiments.

In *Cd27*$^{+/-}$;*Cd70*tg mice, the BM contained significantly fewer B cells, more T cells, and more DCs than in *Cd27*$^{+/-}$ and *Cd27*$^{-/-}$;*Cd70*tg controls (Fig. 6*A*). This altered composition agrees with the B-cell depression and T-cell activation observed in *Cd70*tg mice (23, 24). In *Cd27*$^{+/-}$;*Cd70*tg mice, a proportion of BM-infiltrating B cells, T cells, CD11b^{+} myeloid cells, and DCs expressed CD70 whereas CD70 was not expressed in the *Cd27*$^{+/-}$ controls (Fig. 6*B*). In *Cd27*$^{-/-}$;*Cd70*tg mice, only DCs expressed CD70, and at lower levels than in *Cd27*$^{+/-}$;*Cd70*tg mice (Fig. 6*B*). Therefore, the expression of CD70 on B, T, and CD11b^{+} myeloid cells in *Cd27*$^{+/-}$;CD11c-*Cd70*tg mice was not due to *Cd70* transgene expression, but due to CD27/CD70-driven immune activation. On DCs, CD70 was strongly up-regulated. We conclude that the BM of *Cd27*$^{+/-}$;*Cd70*tg mice is infiltrated with diverse activated immune cells, including DCs that have up-regulated endogenous CD70. OCPs themselves did not express CD70 (Fig. S4*F*).

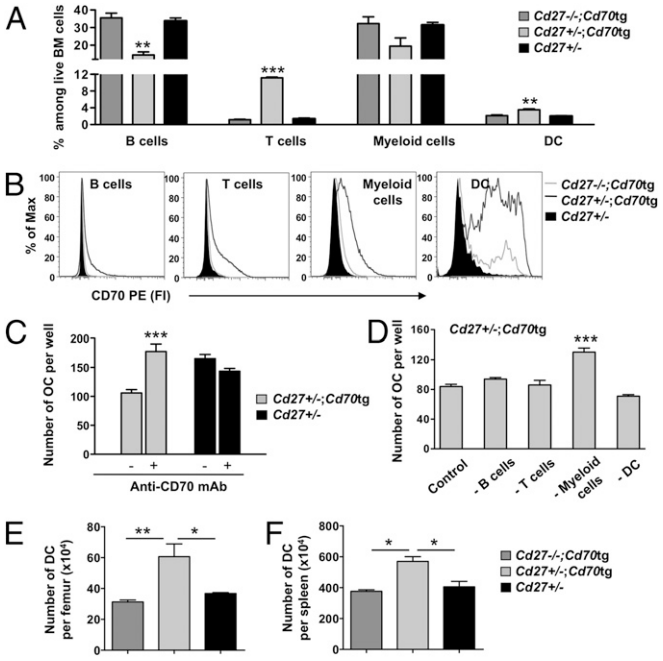

Fig. 6. Constitutive CD27 engagement by CD70-bearing cells in the BM limits OC formation. (*A*) Frequency of B cells (B220$^+$), T cells (CD3$^+$), myeloid cells (CD11b$^+$), and DCs (CD11c$^+$) cells within total BM cells in mice of the indicated genotypes ($n = 3$, age 7–8 wk, $^{**}P < 0.01$; $^{***}P < 0.001$ compared with *Cd27*$^{+/-}$ mice). (*B*) Representative flow cytometric analysis of CD70 expression on the indicated cell populations in the BM of mice of the indicated genotypes, diagnosed as in *A*. Data in *A* and *B* are representative of three independent experiments. (*C*) Numbers of OCs generated from total BM cells of mice of indicated genotypes at day 6 after plating under OC differentiation conditions with (+) or without (–) anti-CD70 mAb FR70 (5 μg/mL). Each bar represents mean ± SEM of four to five mice, with triplicate samples for each mouse ($^{***}P < 0.001$). (*D*) Numbers of OCs formed from total BM cells of *Cd27*$^{+/-}$;*Cd70*tg mice (control) or the same cells that were flow cytometrically depleted for B cells (B220$^+$), T cells (CD3$^+$), myeloid cells (CD11b^{high}), or DCs (CD11c$^+$) ($n = 3$; $^{***}P < 0.001$). Number of cells seeded were corrected for percentage of cells depleted. Data in *C* and *D* are representative of two independent experiments. (*E* and *F*) Absolute number of DCs in BM and spleen of mice of the indicated genotypes ($n = 3$–4, age 7–8 wk; $^{*}P < 0.05$; $^{**}P < 0.01$).

To test whether interactions between CD27 on OCPs and CD70 on surrounding immune cells impeded OC differentiation, we used a well-defined CD70 blocking antibody (28). This antibody restored OC differentiation in *Cd27*$^{+/-}$;*Cd70*tg BM cultures to the level seen in *Cd27*$^{+/-}$ control cultures (Fig. 6*C*), indicating that CD70 caused the inhibition of OC differentiation. We next depleted total BM cells of *Cd27*$^{+/-}$;CD11c-*Cd70*tg mice of B cells, T cells, and CD11b^{high} myeloid cells before OC differentiation cultures. OC formation was not affected by the absence of DCs, indicating that CD70 on DCs was not responsible for the suppression (Fig. 6*D*). However, OC formation was significantly increased in the absence of CD11b^{high} cells, implicating these cells in the observed suppression of OC differentiation via the CD27/CD70 pathway. We considered that, apart from OC differentiation, DC differentiation might also be affected in *Cd27*$^{+/-}$;*Cd70*tg mice, if CD70-bearing immune cells impact on the CD27^{high} OC/DC precursor. Indeed, in BM and spleen of *Cd27*$^{+/-}$;*Cd70*tg mice, DC numbers were significantly increased compared with both controls (Fig. 6 *E* and *F*). This increase suggests that, due to sustained CD27/CD70 interactions, the OC/DC precursor is skewed away from OC differentiation toward DC differentiation (Fig. S6).

Discussion

Arai et al. identified a rare population of c-Kit$^+$CD115$^+$CD11b$^{low/neg}$ cells in the murine BM that is greatly enriched for OCPs (2). These OCPs cannot form granulocytes, megakaryocytes, or erythrocytes, but can form DCs, monocytes, and macrophages (2, 13). They must therefore be downstream from common myeloid precursors and separate from granulocyte/macrophage precursors (29). We have confirmed that the c-Kit$^+$CD115$^+$CD11b^{low} population harbors common OC/DC precursors and have refined that these are in the B220$^-$ fraction, in agreement with Jacquin et al. (26). Moreover, we have discerned among the B220$^-$ c-Kit$^+$CD115$^+$CD11b^{low} population a CD27^{high} subset containing common precursors of OCs, DCs, and macrophages and a downstream, more committed CD27^{low} subset that could yield OCs and macrophages, but not DCs. Upon culture with M-CSF, the CD27^{high} precursors down-regulated CD27 and gained RANK expression, testifying to further OC commitment. The CD27^{low} population was not uniformly RANK$^+$, but contained RANK$^+$ cells, which are likely the previously described RANK$^+$CD115$^+$ quiescent OCPs (27). Moreover Flt3, a key receptor for homeostatic DC differentiation (30) was down-regulated when CD27^{high} OC/DC precursors made the transition to the CD27^{low} stage, indicating further commitment (Fig. S6*B*). However, because CD27^{low} OCPs could still yield macrophages, they were not fully committed to OC differentiation.

The novel field of osteoimmunology highlights that the BM reservoir provides a niche for immune cells to meet OBs, OCs, and their precursors (10, 11). RANKL is made by OBs, but also by certain activated CD4$^+$ T cells, including the proinflammatory T helper-17 subset (12, 31, 32). The cross-talk of these RANKL-bearing T cells with OCPs causes bone loss during chronic immune activation, as in experimental rheumatoid arthritis (12, 32–34). In human, activated T cells likewise drive OC development (35, 36). Based on these findings, Denosumab, a humanized antibody targeting RANKL, was developed for clinical application. Our data now implicate the CD27/CD70 pathway in cross-talk between immune cells and OCPs in the mouse. CD27 deficiency did not affect normal bone homeostasis (Fig. S1), and WT and *Cd27*$^{-/-}$ OCPs differ only in CD27 expression (Fig. S7). Therefore, the CD27/CD70 axis does not appear to control OC development under homeostatic conditions. Rather, our data argue that the CD27/CD70 pathway provides feedback inhibition on OC genesis when activated, CD70$^+$ immune cells infiltrate the BM. Inhibition of OC differentiation in CD11c-*Cd70*tg mice is not due to an intrinsic defect in OCPs or cross-talk among OCPs because purified OCP differentiated normally in vitro. Rather, surrounding cells in the BM cells mediated the suppression, in a CD27/CD70-dependent fashion. Depletion of DCs did not affect OC differentiation, indicating that transgenic CD70 on DCs was not responsible. Rather, activation-induced CD70 on CD11b$^+$ myeloid cells appeared to contribute to the suppression. In CD11c-*Cd70*tg mice, all OCPs have a CD27^{low} phenotype (Fig. 5*A*), presumably due to down-regulation of CD27 by CD70 on surrounding immune cells. However, it is also possible that interaction between CD70 and CD27 on immune cells in the BM results in signals that impact on the OCPs.

CD27-proficient CD11c-*Cd70*tg mice experience progressive immune activation in the first months after birth (24). Most information on immune activation in *Cd70*tg mice has come from analysis of CD19-*Cd70*tg mice that have constitutive CD70 expression on B cells. In these mice, T cells are activated and mature into effector cells that enter into circulation (23). In time, the lymph nodes are depleted of naive T cells whereas B-cell development is arrested by T cell-derived IFNγ (23, 37). This process starts after birth and culminates in a lethal, combined T- and B-cell immunodeficiency. All symptoms are due to sustained CD27–CD70 interactions (37). CD19-*Cd70*tg mice also have an accumulation of OC/DC precursors although they do not display

a bone phenotype (Fig. S8 *A* and *B*). In their BM, primarily the transgenic B cells express CD70, but not CD11b$^+$ cells (Fig. S9). These CD70$^+$ B cells apparently also cause OCP accumulation, but not a bone phenotype. We surmise that the bone phenotype in CD11c-*Cd70*tg mice is due to a niche effect wherein CD70$^+$ CD11b$^+$ cells play an important role. The BM of both *Cd70*tg mouse strains is aberrantly infiltrated with IFNγ-producing T cells (Fig. S10 *A*–*C*). Because IFNγ can inhibit OC differentiation (31), we examined its impact in CD19-*Cd70*tg mice that were available on an IFNγ$^{-/-}$ background. IFNγ deficiency did not rescue the aberrant OCP accumulation in CD19-*Cd70*tg mice (Fig. S10*D*). Therefore, IFNγ produced by activated T cells is most likely not the cause of the OCP accumulation and impaired OC differentiation in CD11c-*Cd70*tg mice.

Thus, under conditions of constitutive CD70 expression on DCs, reflecting chronic immune activation, the CD27/CD70 pathway inhibits OC differentiation and favors DC differentiation. The inhibition of OC genesis consequently provides feedback that can attenuate the detrimental effects of OCs. This feedback may operate during conditions of chronic immune activation that lead to BM infiltration by the relevant CD70-bearing activated immune cells. It will be of interest to find examples of this mechanism in immune-related disease models. In murine collagen-induced arthritis, CD70-blocking antibody attenuated disease, reducing immune cell infiltration of the joints, anti-collagen antibody levels, and bone erosion (38). Thus, the CD27/CD70 pathway promotes rather than inhibits the detrimental effects in arthritis, in line with its driving force in chronic immune activation (18, 23, 24). The *Cd27*$^{+/-}$;CD11c-*Cd70*tg mice also present with lymphopenia, anemia, and increased hematopoiesis in the spleen. In *Cd27*$^{+/+}$;CD19-*Cd70*tg mice, CD27 is down-regulated on hematopoietic stem cells, and leukocyte development from these precursors is impeded (39). Possibly, HSCs are similarly impaired in generating the various blood cell lineages in *Cd27*$^{+/-}$; CD11c-*Cd70*tg mice. The feedback control by CD70$^+$ immune cells on CD27$^+$ hematopoietic precursors in the mouse is consistent and intriguing. We consider therefore that similar mechanisms may play a role in human, where CD27 has recently been detected on CD34$^+$ progenitors in the BM (40). The definition of OCPs used in our study provides a guideline to identify its equivalent in human BM and to examine its regulation by CD70-bearing immune cells.

Materials and Methods

For statistical analysis, the mean ± SEM is depicted in all graphs. For comparisons between two groups, the Student *t* test was used, and, for comparison between multiple groups, the one way ANOVA test was used. For information on mice, procedures for OC isolation, OC differentiation cultures, bone histology and histomorphometry, flow cytometry, and serum analysis, see *SI Materials and Methods*.

ACKNOWLEDGMENTS. We thank F. van Diepen, A. Pfauth, L. Brocks, L. Oomen, and the personnel of the experimental animal and histology facilities of The Netherlands Cancer Institute for excellent services. We thank Dr. J. M. Coquet and T. Schoenmaker for valuable advice and Dr. H. Yagita for the FR70 antibody.

1. Pittenger MF, et al. (1999) Multilineage potential of adult human mesenchymal stem cells. *Science* 284(5411):143–147.
2. Arai F, et al. (1999) Commitment and differentiation of osteoclast precursor cells by the sequential expression of c-Fms and receptor activator of nuclear factor kappaB (RANK) receptors. *J Exp Med* 190(12):1741–1754.
3. Quinn JM, Elliott J, Gillespie MT, Martin TJ (1998) A combination of osteoclast differentiation factor and macrophage-colony stimulating factor is sufficient for both human and mouse osteoclast formation in vitro. *Endocrinology* 139(10):4424–4427.
4. Lacey DL, et al. (1998) Osteoprotegerin ligand is a cytokine that regulates osteoclast differentiation and activation. *Cell* 93(2):165–176.
5. Kong YY, et al. (1999) OPGL is a key regulator of osteoclastogenesis, lymphocyte development and lymph-node organogenesis. *Nature* 397(6717):315–323.
6. Kim N, Odgren PR, Kim DK, Marks SC, Jr., Choi Y (2000) Diverse roles of the tumor necrosis factor family member TRANCE in skeletal physiology revealed by TRANCE deficiency and partial rescue by a lymphocyte-expressed TRANCE transgene. *Proc Natl Acad Sci USA* 97(20):10905–10910.
7. Fuller K, Wong B, Fox S, Choi Y, Chambers TJ (1998) TRANCE is necessary and sufficient for osteoblast-mediated activation of bone resorption in osteoclasts. *J Exp Med* 188(5):997–1001.
8. Yasuda H, et al. (1998) Osteoclast differentiation factor is a ligand for osteoprotegerin/osteoclastogenesis-inhibitory factor and is identical to TRANCE/RANKL. *Proc Natl Acad Sci USA* 95(7):3597–3602.
9. Nakashima T, et al. (2011) Evidence for osteocyte regulation of bone homeostasis through RANKL expression. *Nat Med* 17(10):1231–1234.
10. Takayanagi H (2007) Osteoimmunology: Shared mechanisms and crosstalk between the immune and bone systems. *Nat Rev Immunol* 7(4):292–304.
11. Walsh MC, et al. (2006) Osteoimmunology: Interplay between the immune system and bone metabolism. *Annu Rev Immunol* 24:33–63.
12. Kong YY, et al. (1999) Activated T cells regulate bone loss and joint destruction in adjuvant arthritis through osteoprotegerin ligand. *Nature* 402(6759):304–309.
13. Miyamoto T, et al. (2001) Bifurcation of osteoclasts and dendritic cells from common progenitors. *Blood* 98(8):2544–2554.
14. Wiesmann A, et al. (2000) Expression of CD27 on murine hematopoietic stem and progenitor cells. *Immunity* 12(2):193–199.
15. Medina KL, et al. (2001) Identification of very early lymphoid precursors in bone marrow and their regulation by estrogen. *Nat Immunol* 2(8):718–724.
16. Serwold T, Ehrlich LI, Weissman IL (2009) Reductive isolation from bone marrow and blood implicates common lymphoid progenitors as the major source of thymopoiesis. *Blood* 113(4):807–815.
17. Franco CB, Chen CC, Drukker M, Weissman IL, Galli SJ (2010) Distinguishing mast cell and granulocyte differentiation at the single-cell level. *Cell Stem Cell* 6(4):361–368.
18. Nolte MA, van Olffen RW, van Gisbergen KP, van Lier RA (2009) Timing and tuning of CD27-CD70 interactions: The impact of signal strength in setting the balance between adaptive responses and immunopathology. *Immunol Rev* 229(1):216–231.
19. Borst J, Hendriks J, Xiao Y (2005) CD27 and CD70 in T cell and B cell activation. *Curr Opin Immunol* 17(3):275–281.
20. van Montfrans JM, et al. (2012) CD27 deficiency is associated with combined immunodeficiency and persistent symptomatic EBV viremia. *J Allergy Clin Immunol* 129(3):787–793.
21. Lee WW, Yang ZZ, Li G, Weyand CM, Goronzy JJ (2007) Unchecked CD70 expression on T cells lowers threshold for T cell activation in rheumatoid arthritis. *J Immunol* 179(4):2609–2615.
22. Han BK, et al. (2005) Increased prevalence of activated CD70+CD4+ T cells in the periphery of patients with systemic lupus erythematosus. *Lupus* 14(8):598–606.
23. Arens R, et al. (2001) Constitutive CD27/CD70 interaction induces expansion of effector-type T cells and results in IFNgamma-mediated B cell depletion. *Immunity* 15(5):801–812.
24. Keller AM, Schildknecht A, Xiao Y, van den Broek M, Borst J (2008) Expression of costimulatory ligand CD70 on steady-state dendritic cells breaks CD8+ T cell tolerance and permits effective immunity. *Immunity* 29(6):934–946.
25. de Vries TJ, Schoenmaker T, Beertsen W, van der Neut R, Everts V (2005) Effect of CD44 deficiency on in vitro and in vivo osteoclast formation. *J Cell Biochem* 94(5):954–966.
26. Jacquin C, Gran DE, Lee SK, Lorenzo JA, Aguila HL (2006) Identification of multiple osteoclast precursor populations in murine bone marrow. *J Bone Miner Res* 21(1):67–77.
27. Muto A, et al. (2011) Lineage-committed osteoclast precursors circulate in blood and settle down into bone. *J Bone Miner Res* 26(12):2978–2990.
28. Oshima H, et al. (1998) Characterization of murine CD70 by molecular cloning and mAb. *Int Immunol* 10(4):517–526.
29. Weissman IL, Shizuru JA (2008) The origins of the identification and isolation of hematopoietic stem cells, and their capability to induce donor-specific transplantation tolerance and treat autoimmune diseases. *Blood* 112(9):3543–3553.
30. Adolfsson J, et al. (2005) Identification of Flt3+ lympho-myeloid stem cells lacking erythro-megakaryocytic potential a revised road map for adult blood lineage commitment. *Cell* 121(2):295–306.
31. Takayanagi H, et al. (2000) T-cell-mediated regulation of osteoclastogenesis by signalling cross-talk between RANKL and IFN-gamma. *Nature* 408(6812):600–605.
32. Sato K, et al. (2006) Th17 functions as an osteoclastogenic helper T cell subset that links T cell activation and bone destruction. *J Exp Med* 203(12):2673–2682.
33. Pettit AR, et al. (2001) TRANCE/RANKL knockout mice are protected from bone erosion in a serum transfer model of arthritis. *Am J Pathol* 159(5):1689–1699.
34. Lubberts E, et al. (2000) IL-4 gene therapy for collagen arthritis suppresses synovial IL-17 and osteoprotegerin ligand and prevents bone erosion. *J Clin Invest* 105(12):1697–1710.
35. Kotake S, et al. (2001) Activated human T cells directly induce osteoclastogenesis from human monocytes: possible role of T cells in bone destruction in rheumatoid arthritis patients. *Arthritis Rheum* 44(5):1003–1012.
36. Kotake S, et al. (2005) IFN-gamma-producing human T cells directly induce osteoclastogenesis from human monocytes via the expression of RANKL. *Eur J Immunol* 35(11):3353–3363.
37. Tesselaar K, et al. (2003) Lethal T cell immunodeficiency induced by chronic costimulation via CD27-CD70 interactions. *Nat Immunol* 4(1):49–54.
38. Oflazoglu E, et al. (2009) Blocking of CD27-CD70 pathway by anti-CD70 antibody ameliorates joint disease in murine collagen-induced arthritis. *J Immunol* 183(6): 3770–3777.
39. Nolte MA, et al. (2005) Immune activation modulates hematopoiesis through interactions between CD27 and CD70. *Nat Immunol* 6(4):412–418.
40. Schürch C, Riether C, Matter MS, Tzankov A, Ochsenbein AF (2012) CD27 signaling on chronic myelogenous leukemia stem cells activates Wnt target genes and promotes disease progression. *J Clin Invest* 122(2):624–638.